

High Conversion Efficiency in Multi-mode Gas-filled Hollow-core Fiber

Md. Selim Habib, *Senior Member, IEEE, Member, OSA*, Christos Markos, *Member, OSA*, and Rodrigo Amezcua-Correa, *Member, OSA*

Abstract—In this letter, an energetic and highly efficient dispersive wave (DW) generation at 200 nm has been numerically demonstrated by selectively exciting LP₀₂-like mode in a 10 bar Ar-filled hollow-core anti-resonant fiber pumping in the anomalous dispersion regime at 1030 nm with pulses of 30 fs duration and 7 μJ energy. Our calculations indicate high conversion efficiency of >35% (2.5 μJ) after propagating 3.6 cm fiber length which is due to the strong shock effect and plasma induced blue-shifted soliton. It is observed that the efficiency of fundamental LP₀₁-mode is about 15% which is much smaller than LP₀₂-like mode and also emitted at longer wavelength of 270 nm.

Index Terms—Hollow-core anti-resonant fiber, ultrafast nonlinear dynamics, higher-order mode, dispersive wave.

I. INTRODUCTION

THE ultraviolet (UV) spectral range (100-400 nm) is of great interest in the scientific community because of wide range of applications such as spectroscopy [1], control of chemical reactions [2], biomedicine [3], and femtosecond (fs) pump-probe measurements [4]. Despite of numerous applications, the availability of such UV sources in this spectral regime are limited and a very few laser sources directly emit UV light and some require complex set-up [5]. These UV laser sources include excimer lasers [6], cerium fluoride lasers [7], harmonic generation [8], and diode lasers [9]. Recently, hollow-core anti-resonant fibers (HC-ARFs) offer many appealing features including broadband guidance, low-light glass overlap, low propagation loss, and weak anomalous dispersion to study ultrafast nonlinear dynamics when filled with noble gases [10]–[15]. One of the remarkable features of adding gas in HC-ARF is that both the dispersion landscape and nonlinearity can be tuned by simply changing the pressure of the gas. Based on these properties, several impressive results have been reported to generate light in the UV [5], [11]–[13]. However most of the works on the UV light generation have been performed considering the excitation of a pure LP₀₁-like mode and it is relied on a well-known process called soliton self-compression to the sub single-cycle regime, followed by resonant DW radiation [10]. For example, bright emission of

UV light was first theoretically predicted in an Ar-filled HC-ARF with efficiency of 20% [16] and later experimentally reported with efficiency of 6% [11]. Recently, an energetic DW generation at 275 nm is experimentally demonstrated by pumping in the mid-IR regime of 2460 nm [12].

In this work, blue-shifted DW generation with high conversion efficiency at around 200 nm has been demonstrated by exciting LP₀₂-like mode in an uniform Ar-filled HC-ARF with experimentally feasible fiber and pulse parameters. The generated DW has an efficiency of >35% when the fiber is filled under 10 bar Ar, pumped in the anomalous dispersion regime of 1030 nm, 30 fs pulse duration, and 7 μJ pulse energy. The high efficiency of the generated DW wave is due to the combination of self-phase modulation and anomalous dispersion, extreme shock effect and plasma-induced blue-shifted soliton. The temporal pulse is compressed down to less than single cycle of ~1.5 fs. In comparison, the the nonlinear dynamics of LP₀₁-like mode is also investigated. When a LP₀₁-like mode is excited, the DW emits at a longer wavelength of ~270 nm with efficiency of 15%. However, the compressed pulse is not sufficient to ionize the gas due to the lack of sufficient free electron generation.

II. FIBER MODELING AND MODAL DISPERSION

The HC-ARF considered in this work consists of 10-nested tubes with a core diameter of 40 μm, wall thickness of 300 nm, gap separation of 2 μm, and nested tube tube ratio, $d/D = 0.5$. The wall thickness of 300 nm provides the center of first-order resonance at 630 nm calculated using [17]: $\lambda_r = \frac{2t}{m} \sqrt{(n_g^2 - 1)}$, where t is the wall thickness, n_g is the refractive index of silica glass, and m is the resonance order. The wall thickness is chosen 300 nm such that the resonance is far away from the laser pump wavelength of 1030 nm. The modal properties of the fiber was calculated using finite-element (FE) modeling based on COMSOL[®] software according to [17]–[19]. The HC-ARF can be designed multi-mode by carefully engineering the cladding parameters and number of tubes [18]. The fiber is shown in Fig. 1(a) which can support more than 20 spatial modes and has maximum threshold loss of <100 dB/km. Fig. 1(a) shows the mode-field profiles of LP₀₁ and LP₀₂-like modes which are well confined in the core and the loss of these modes are <10 dB/km at the pump wavelength of 1030 nm.

The propagation constant of LP _{mn} -like mode of HC-ARF can be represented using a capillary model [21]:

Manuscript received August XX, 2021.

M. Selim Habib is with the Department of Electrical and Computer Engineering, Florida Polytechnic University, FL-33805, USA (e-mail: mhabib@floridapoly.edu).

C. Markos is with the Department of Photonics Engineering, Technical University of Denmark, DK-2800, Denmark (e-mail: chmar@fotonik.dtu.dk).

R. Amezcua-Correa is with CREOL, University of Central Florida, FL-32826, USA (e-mail: r.amezcua@creol.ucf.edu).

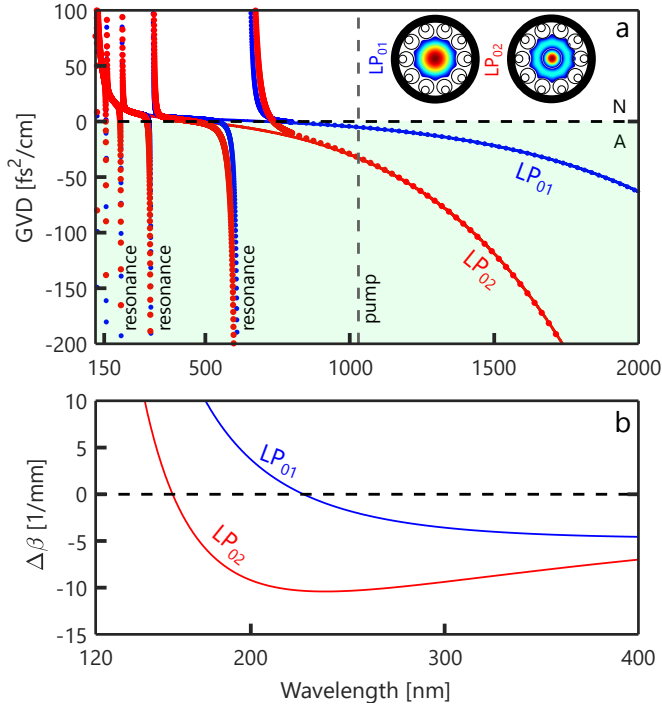


Fig. 1. Numerically calculated (a) GVD of LP₀₁ (blue) and LP₀₂ (red)-like mode using modified capillary model [20] and FM modeling. solid: modified capillary model; dotted: FM modeling. The fiber has a core diameter of 40 μm, wall thickness of 300 nm, gap separation of 2 μm, and nested tube ratio of 0.5. The definition of fiber geometrical parameters can be found in [19]. Inset of (a): mode-field profile of LP₀₁ and LP₀₂-like mode. (b) propagation constant mismatch Δβ between soliton and DW according to [10]. The contribution of ionization is not included. N: normal and A: anomalous dispersion. The light green shaded area presents the anomalous dispersion regime.

$$\beta_{mn}(\omega) = \sqrt{\frac{\omega^2 n_{\text{gas}}^2(\omega, p)}{c^2} - \frac{U_{mn}^2}{R_{\text{eff}}^2}}, \quad (1)$$

where ω is the angular frequency, c is the velocity of light in vacuum, $n_{\text{gas}}(\omega, p)$ is the frequency and pressure dependent refractive index of the filling gas calculated using [22], U_{mn} is the n th zero of the m th-order Bessel function of the first kind (LP₀₁-like mode: $U_{01} = 2.450$ and LP₀₂-like mode: $U_{02} = 5.520$), R_{eff} is the effective core radius according to [20]. The group velocity dispersion (GVD) of a 40 μm HC-ARF under 10 bar Ar was calculated using the capillary model which has been extensively used to study the ultrafast nonlinear dynamics in gas-filled fiber systems [23]–[26]. In comparison, the GVD was also calculated using FE modeling and it is seen from Fig. 1(a) that both models agrees very well. The only difference between the two models is that FE modeling can track the resonance bands which are determined by the fiber wall thickness. The zero-dispersion wavelength of LP₀₁ and LP₀₂-like modes are 712 nm and 481 nm respectively. At the pump wavelength, the calculated GVD of LP₀₁ and LP₀₂-like modes are -4.95 fs²/cm and -32.91 fs²/cm respectively. The phase mismatch ($\Delta\beta$) between the soliton and dispersive wave (DW) of LP₀₁ and LP₀₂-like modes are shown in Fig. 1(b). The phase mismatch was

calculated according to [10] neglecting the ionization effect. It can be seen from Fig. 1(b) that the DW of a pure LP₀₂-like mode is blue shifted compared to the LP₀₁-like mode since the zero-dispersion wavelength of LP₀₂-like mode resides in the blue side.

III. PULSE PROPAGATION EQUATION

The optical pulse propagation was studied using a unidirectional pulse propagation equation which includes free-electron effects but without considering polarization and coupling between the different modes can be expressed as [23]–[25]:

$$\begin{aligned} \partial_z E(z, \omega) = & i\beta_{mn}(\omega - \frac{\omega}{v_g})E(z, \omega) + i\frac{\omega^2}{\mu_0} \mathcal{F} \left\{ \epsilon_0 \chi^{(3)} E(z, t)^3 \right\} \\ & - \frac{\omega \epsilon_0}{2\beta(\omega)} \mathcal{F} \left\{ \partial_t \rho(z, t) \frac{I_p}{E(z, t)} + \frac{e^2}{m_e} \int_{-\infty}^t \rho(z, t') E(z, t') \right\}, \end{aligned} \quad (2)$$

where z is the propagation direction, t is the time in the reference frame moving with the pump group velocity v_g , $E(z, \omega)$ is the electric field in the frequency domain, $\beta_{mn}(\omega)$ is the propagation constant, ϵ_0 and μ_0 are the permittivity and permeability of free space respectively, $\chi^{(3)}$ is the third order susceptibility, ρ is the time varying free electron (plasma) density, I_p is the first ionization energy, e and m_e are the charge and mass of electron respectively, and \mathcal{F} denotes the Fourier transform. The Raman contribution of silica was neglected due to the very low light–glass overlap ($\ll 1\%$) and we assume nonradial dependence of plasma. A quasi-static tunneling based on Ammosov, Delone, and Krainov (ADK) model was used to calculate the plasma density [27].

IV. NUMERICAL RESULTS AND DISCUSSIONS

The spectral and temporal evolution of LP₀₁ and LP₀₂-like mode in a 10 cm long fiber filled with 10 bar Ar, pumped at 1030 nm with 30 fs pulse and pulse energy of 7 μJ is shown in Fig. 2. We begin our analyses by considering the excitation of LP₀₁-like mode. For fundamental LP₀₁-like mode, the pulse undergoes soliton self-compression down to ~ 3.5 fs with peak intensity > 65 TW/cm² after propagating ~ 5.5 cm due to the interplay between self-phase modulation and anomalous dispersion. At the maximum compression point, a DW is emitted at ~ 270 nm in the normal dispersion regime and a supercontinuum generation (SC) spanning 270–1800 nm. However, the peak intensity of the compressed pulse was not enough to ionize the gas since the plasma density at the maximum temporal compression point was found around 10^{14} cm⁻³ (see Fig. 4(b)). Therefore, a similar spectral and temporal evolution can be seen when the ionization effect is turned-off which is not shown in Fig. 2.

For LP₀₂-like mode, the pulse undergoes a strong soliton self-compression down to ~ 1.5 fs (less than a single cycle) with peak intensity > 220 TW/cm² at an early stage of ~ 3.6 cm, and a strong DW is emitted at 200 nm. Such a high intense pulse is enough to ionize the gas and form a plasma and a blue-shifted soliton (BSF) appears in the spectral profile. Unlike the SC of LP₀₁-like mode, the SC of LP₀₂-like mode

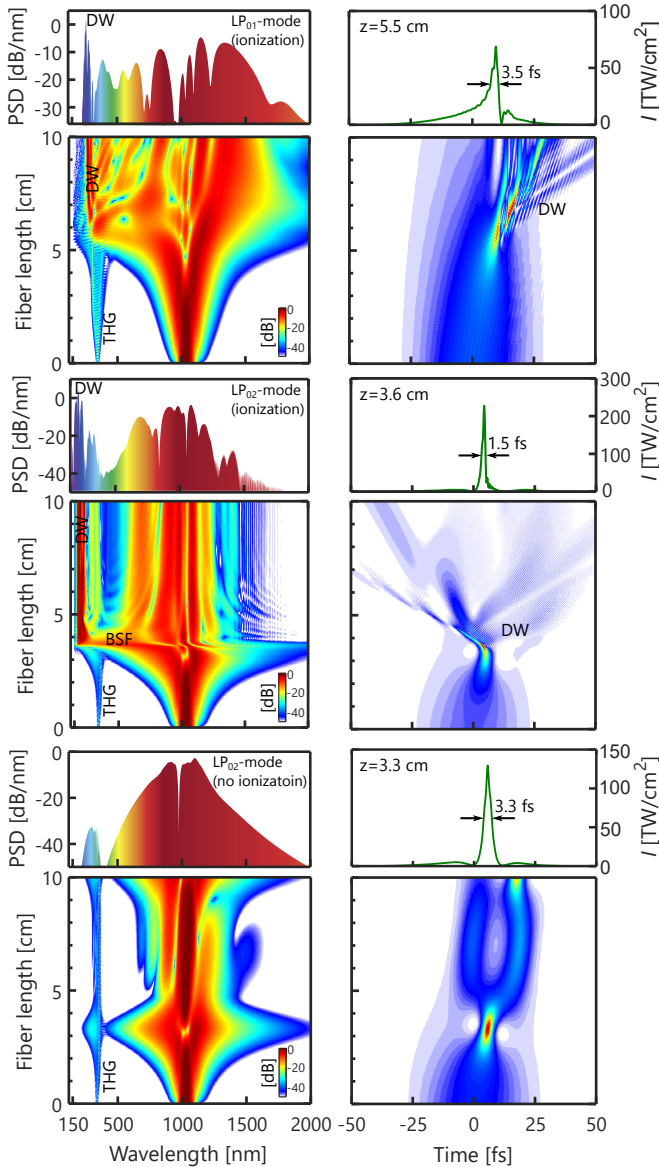


Fig. 2. Numerically simulated spectral (left) and temporal (right) evolution for a 40 μm core HC-ARF under 10 bar of Ar, pulse energy of 7 μJ , pulse duration of 30 fs, and 1030 nm pump wavelength. Spectral and temporal evolution of LP₀₁-like mode with ionization (top row), LP₀₂-like mode with ionization (middle row), LP₀₂-like mode without ionization (bottom row). The fiber has a wall thickness of 300 nm, gap separation of 2 μm , and nested tube ratio of 0.5. BSF: blue-shifted soliton, THG: third-harmonic generation. The simulations were performed using modified capillary model [20]. The PSD was calculated using: $\text{PSD} = \frac{c}{\lambda^2} |E(z, \lambda)|^2 f_{\text{rep}}$, where f_{rep} is the laser repetition rate.

is narrower at the longer wavelengths that can be seen after the temporal compression which is due to the high ionization loss [28]. The spectral and temporal evolution of LP₀₂-like mode without ionization is shown in Fig. 2 (bottom row). When the ionization effect was not considered, DW is not generated in the UV regime since the energy of the compressed pulse is not sufficient to phase match to the DW. It turns out that the ionization effect is responsible for the generation of DW for LP₀₂-like mode and plays an important role of DW generation.

To confirm the DW emission of LP₀₂-like mode at 200 nm,

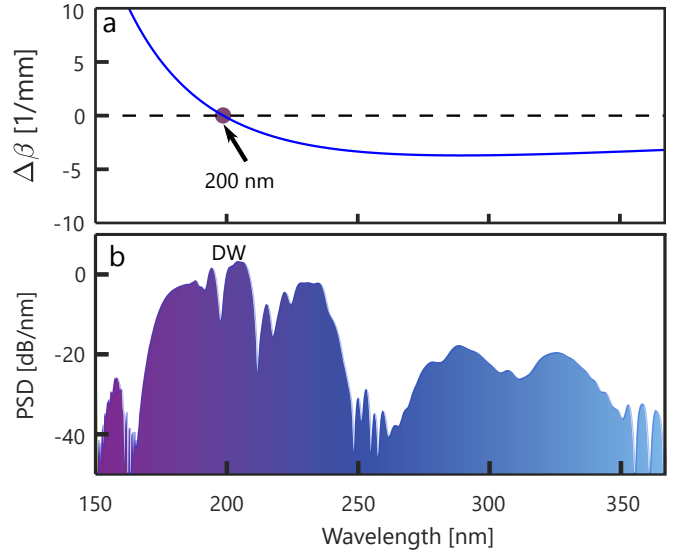


Fig. 3. (a) Phase mismatch ($\Delta\beta$) between a soliton and DW for LP₀₂-like mode according to [26]. The 40 μm HC-ARF was filled with 10 bar Ar, pumped at 1030 nm with a pulse energy of 7 μJ and 30 fs pulse duration. The ionization was included to calculate the phase mismatch. The plasma density of $> 10^{18} \text{ cm}^{-3}$ is calculated at maximum temporal compression. (b) The normalized PSD with UV dispersive wave emission.

the phase mismatch curve ($\Delta\beta$) between the soliton and the DW including the ionization effect is shown in Fig. 3(a). The phase mismatch can be expressed as [26]:

$$\Delta\beta = \beta(\omega) - \left(\beta_0 + \frac{1}{v_g}[\omega - \omega_0] + \gamma P_p \frac{\omega}{\omega_0} - \frac{\omega_0}{2n_0 c} \frac{\rho}{\rho_{cr}} \frac{\omega_0}{\omega} \right), \quad (3)$$

where β_0 is the propagation constant at the soliton centre frequency ω_0 , γ is the nonlinear fiber parameter at the pump wavelength [10], P_p is the soliton peak power of the compressed pulse, n_0 is the linear refractive index of the medium, $\rho_{cr} \equiv \epsilon_0 m_e \frac{\omega_0^2}{c^2}$ is the critical plasma density [29]. It can be seen from Fig. 3(a) that the phase matching occurs at 200 nm which agrees well with the DW wave emission seen from the power spectral density (PSD) curve of Fig. 3(b). It should be noted that when the ionization effect is considered the phase matching condition occurred at longer wavelengths since the pump soliton shifts toward the blue side [28] (see Fig. 2 (middle row)).

The DW efficiency and plasma density of LP₀₁ and LP₀₂-like modes are shown in Fig. 4(a-b). The DW efficiency of LP₀₂-like mode is $>35\%$ whereas the efficiency of LP₀₁-like mode is around 15%. The dramatic enhancement of the DW emission for LP₀₂-like mode is due to the strong shock effect and ionization-induced blue-shift [28]. The plasma density of LP₀₂-like mode is above $>10^{18} \text{ cm}^{-3}$ at the maximum temporal compression point which is enough to ionize the gas. The free electron generation decays drastically after the temporal compression as it propagates through the fiber due to the high ionization loss. However, at the temporal compression point, the plasma density of LP₀₁-like mode is only 10^{14} cm^{-3} .

To get more physical insights on the underlying mechanism

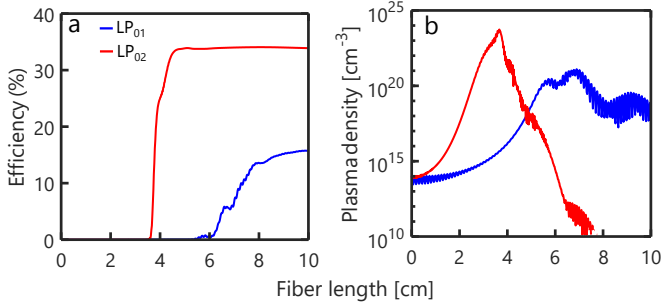


Fig. 4. Efficiency (a) and average plasma density along the fiber propagation distance for LP₀₁ (blue) and LP₀₂ (red)-like mode. The maximum efficiency of LP₀₁ is >35% whereas for LP₀₂-like mode is ~15 %. The plasma density was calculated using [24], [27].

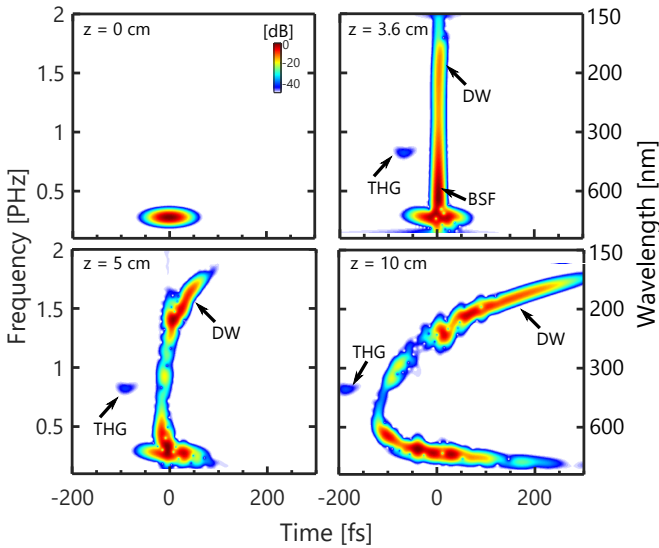


Fig. 5. Calculated spectrogram of LP₀₂-like mode for a 40 μm core HC-ARF under 10 bar of Ar, pulse energy 7 μJ , pulse duration 30 fs, and 1030 nm pump wavelength at selected distances. The ionization is included in the simulation. The spectrogram was calculated using a 10 fs Gaussian gate pulse. The third harmonic of the pump pulse is evident at 343.33 nm.

of DW emission for the LP₀₂-like mode, the spectrograms are plotted in Fig. 5 using the cross correlation frequency-resolved optical gating for different selected fiber lengths. A 10 fs Gaussian pulse were used to plot these spectrograms. The location of DW, blue-shifted soliton (BSF), third-harmonic generation (THG) are shown. At the propagation distance of $z = 3.6$ cm, the pulse undergoes a maximum temporal compression and the spectrum extends towards the blue due to the plasma formation and a DW is emitted in the normal dispersion regime at around 200 nm. During the propagation, the DWs broadens linearly in time which can be seen for $z = 5$ cm and $z = 10$ cm.

V. CONCLUSION

In conclusion, a new approach to enhance the efficiency of a DW generated in the UV regime by exciting LP₀₂-like mode in Ar-filled HC-ARF has been demonstrated. The numerical modelings are based on the experimentally feasible fiber and pulse parameters that can predict DW generation at 200 nm

followed by SC spanning 200–1500 nm. The formation of extreme shock effect and plasma induced blue-shifted soliton leads to an efficiency of >35%. The numerical modeling predicts that it requires only 3.6 cm of fiber to generate the DW. The DW can be further blue-shifted if higher LP_{0n} are excited but requires more pump energy to phase match the soliton and DW. The results presented in this work may be valuable towards the development of compact, bright, and highly efficient UV light source.

REFERENCES

- [1] F. Reinert and S. Hüfner, “Photoemission spectroscopy—from early days to recent applications,” *New Journal of Physics*, vol. 7, no. 1, p. 97, 2005.
- [2] M. C. Asplund, P. T. Snee, J. S. Yeston, M. J. Wilkens, C. K. Payne, H. Yang, K. T. Kotz, H. Frei, R. G. Bergman, and C. B. Harris, “Ultrafast UV pump/IR probe studies of C-H activation in linear, cyclic, and aryl hydrocarbons,” *Journal of the American Chemical Society*, vol. 124, no. 35, pp. 10605–10612, 2002.
- [3] R. Steiner, “Medical applications of mid-ir solid-state lasers,” in *Mid-infrared coherent sources and applications*. Springer, 2008, pp. 575–588.
- [4] P. Hockett, C. Z. Bisgaard, O. J. Clarkin, and A. Stolow, “Time-resolved imaging of purely valence-electron dynamics during a chemical reaction,” *Nature Physics*, vol. 7, no. 8, pp. 612–615, 2011.
- [5] F. Köttig, F. Tani, C. M. Biersach, J. C. Travers, and P. S. J. Russell, “Generation of microjoule pulses in the deep ultraviolet at megahertz repetition rates,” *Optica*, vol. 4, no. 10, pp. 1272–1276, 2017.
- [6] J. J. Ewing, “Rare-gas halide lasers,” *Physics Today*, vol. 31, no. 5, pp. 32–39, 1978.
- [7] E. Granados, D. W. Coutts, and D. J. Spence, “Mode-locked deep ultraviolet ce: Licaf laser,” *Optics letters*, vol. 34, no. 11, pp. 1660–1662, 2009.
- [8] J. Rothhardt, C. Rothhardt, M. Müller, A. Klenke, M. Kienel, S. Demmler, T. Elsmann, M. Rothhardt, J. Limpert, and A. Tünnermann, “100 w average power femtosecond laser at 343 nm,” *Optics letters*, vol. 41, no. 8, pp. 1885–1888, 2016.
- [9] Z. Zhang, M. Kushimoto, T. Sakai, N. Sugiyama, L. J. Schowalter, C. Sasaoka, and H. Amano, “A 271.8 nm deep-ultraviolet laser diode for room temperature operation,” *Applied Physics Express*, vol. 12, no. 12, p. 124003, 2019.
- [10] J. C. Travers, W. Chang, J. Nold, N. Y. Joly, and P. S. J. Russell, “Ultrafast nonlinear optics in gas-filled hollow-core photonic crystal fibers,” *JOSA B*, vol. 28, no. 12, pp. A11–A26, 2011.
- [11] N. Y. Joly, J. Nold, W. Chang, P. Hölzer, A. Nazarkin, G. Wong, F. Biancalana, and P. S. J. Russell, “Bright spatially coherent wavelength-tunable deep-UV laser source using an Ar-filled photonic crystal fiber,” *Physical Review Letters*, vol. 106, no. 20, p. 203901, 2011.
- [12] A. I. Adamu, M. S. Habib, C. R. Petersen, J. E. A. Lopez, B. Zhou, A. Schülzgen, M. Bache, R. Amezcua-Correa, O. Bang, and C. Markos, “Deep-UV to mid-ir supercontinuum generation driven by mid-ir ultrashort pulses in a gas-filled hollow-core fiber,” *Scientific reports*, vol. 9, no. 1, pp. 1–9, 2019.
- [13] A. I. Adamu, M. S. Habib, C. R. Smith, J. E. A. Lopez, P. U. Jepsen, R. Amezcua-Correa, O. Bang, and C. Markos, “Noise and spectral stability of deep-UV gas-filled fiber-based supercontinuum sources driven by ultrafast mid-IR pulses,” *Scientific reports*, vol. 10, no. 1, pp. 1–10, 2020.
- [14] C. Markos, J. C. Travers, A. Abdolvand, B. J. Eggleton, and O. Bang, “Hybrid photonic-crystal fiber,” *Reviews of Modern Physics*, vol. 89, no. 4, p. 045003, 2017.
- [15] M. S. Habib, C. Markos, O. Bang, and M. Bache, “Soliton-plasma nonlinear dynamics in mid-IR gas-filled hollow-core fibers,” *Optics letters*, vol. 42, no. 11, pp. 2232–2235, 2017.
- [16] S.-J. Im, A. Husakou, and J. Herrmann, “High-power soliton-induced supercontinuum generation and tunable sub-10-fs VUV pulses from kagome-lattice HC-PCFs,” *Optics express*, vol. 18, no. 6, pp. 5367–5374, 2010.
- [17] F. Poletti, “Nested antiresonant nodeless hollow core fiber,” *Optics express*, vol. 22, no. 20, pp. 23807–23828, 2014.
- [18] M. S. Habib, J. Antonio-Lopez, C. Markos, A. Schülzgen, and R. Amezcua-Correa, “Single-mode, low loss hollow-core anti-resonant fiber designs,” *Optics express*, vol. 27, no. 4, pp. 3824–3836, 2019.

- [19] M. S. Habib, C. Markos, and R. Amezcua-Correa, "Impact of cladding elements on the loss performance of hollow-core anti-resonant fibers," *Optics Express*, vol. 29, no. 3, pp. 3359–3374, 2021.
- [20] M. I. Hasan, N. Akhmediev, and W. Chang, "Empirical formulae for dispersion and effective mode area in hollow-core antiresonant fibers," *Journal of Lightwave Technology*, vol. 36, no. 18, pp. 4060–4065, 2018.
- [21] E. A. Marcatili and R. Schmelzter, "Hollow metallic and dielectric waveguides for long distance optical transmission and lasers," *Bell System Technical Journal*, vol. 43, no. 4, pp. 1783–1809, 1964.
- [22] A. Börzsönyi, Z. Heiner, M. Kalashnikov, A. Kovács, and K. Osvay, "Dispersion measurement of inert gases and gas mixtures at 800 nm," *Applied optics*, vol. 47, no. 27, pp. 4856–4863, 2008.
- [23] W. Chang, A. Nazarkin, J. Travers, J. Nold, P. Hölzer, N. Joly, and P. S. J. Russell, "Influence of ionization on ultrafast gas-based nonlinear fiber optics," *Optics express*, vol. 19, no. 21, pp. 21 018–21 027, 2011.
- [24] W. Chang, P. Hölzer, J. Travers, and P. S. J. Russell, "Combined soliton pulse compression and plasma-related frequency upconversion in gas-filled photonic crystal fiber," *Optics letters*, vol. 38, no. 16, pp. 2984–2987, 2013.
- [25] D. Novoa, M. Cassataro, J. C. Travers, and P. S. J. Russell, "Photoionization-induced emission of tunable few-cycle midinfrared dispersive waves in gas-filled hollow-core photonic crystal fibers," *Physical review letters*, vol. 115, no. 3, p. 033901, 2015.
- [26] F. Köttig, D. Novoa, F. Tani, M. C. Günendi, M. Cassataro, J. Travers, and P. S. J. Russell, "Mid-infrared dispersive wave generation in gas-filled photonic crystal fibre by transient ionization-driven changes in dispersion," *Nature communications*, vol. 8, no. 1, pp. 1–8, 2017.
- [27] M. V. Ammosov, "Tunnel ionization of complex atoms and of atomic ions in an alternating electromagnetic field," *Sov. Phys. JETP*, vol. 64, p. 1191, 1987.
- [28] M. F. Saleh, W. Chang, P. Hölzer, A. Nazarkin, J. C. Travers, N. Y. Joly, P. S. J. Russell, and F. Biancalana, "Theory of photoionization-induced blueshift of ultrashort solitons in gas-filled hollow-core photonic crystal fibers," *Physical Review Letters*, vol. 107, no. 20, p. 203902, 2011.
- [29] A. Couairon and A. Mysyrowicz, "Femtosecond filamentation in transparent media," *Physics reports*, vol. 441, no. 2-4, pp. 47–189, 2007.